PROC. OF JSCE,
No. 280, DEC. 1978

STRESS-STRAIN RELATIONSHIPS OF SAND BASED ON ELASTO-PLASTICITY THEORY

By Koichi NISHI and Yasuyuki ESASHI***

1. INTRODUCTION

Bearing capacity and deformation analyses of the ground and foundations in terms of numerical technique represented by finite element method have become as one of the recent topics in the field of soil mechanics. Various boundary value problems have been solved by means of these technique and a number of excellent findings have been given for the design and construction of foundations.

In general, non linear elastic analyses are often carried out by varying deformation modulus depending on the stress level (for example, see Duncan and Chang[6]). However, soils show the inherent characteristics such as dilatancy and stress path dependency during shear deformation. Also, intermediate principal stress and strain history influence largely on deformation behaviour and strength of soils.

On the other hand, from the view of theory of plasticity, stress-strain relationships for soils have been advanced by some researchers.

Research group leading Roscoe (Roscoe, Schofield and Thurayrajah[20]; Schofield and Wroth[22]; Roscoe and Burland[21]) developed new theories on the deformation behaviour of soil materials by inducing the concept of normality rule in theory of plasticity.

On the other hand, Poorooshasb, Holubec and Sherbourne[17),18)], Poorooshasb[19)], and Lade and Duncan[10] proposed stress strain relationships of sand by using non associated flow rule.

Based on the microscopic view point, Murayama[16)] derived theoretically hyperbolic type's stress strain relations. Matsuoka[11)] proposed spatial mobilized plane and developed Murayama's theory to generalized stress strain relationships. Barden and Khayatt[3)] and Barden, Ismail and Tong[4)] induced plastic potential under various stress conditions based on Rowe's stress dilatancy theory.

In such way, the studies on the deformation properties of sand have been advanced from various standpoints. Particularly, the theory of Roscoe et al. was expanded by some investigators (for example, Adachi and Okano[1)]) to generalized stress conditions and it has been applied to some boundary value problems (for example, Simpson and Wroth[24)]). However, deformation theories that can exactly describe strain history and dilatancy characteristic that contracts initially and expands at prepeak in shear deformation, are not be founded.

In this study, sand is regarded as work hardening material with dilatancy, and yield function, hardening function and plastic potential are proposed from the experimental evidences and theoretical considerations. Finally, stress strain relationships under generalized stress conditions will be constructed based on elasto-plasticity theory.

2. PREVIOUS REVIEW AND DISCUSSION ON YIELDING PROPERTIES OF SAND

Experimental study on yielding properties of sand was carried out in the first place by Poorooshasb et al.[17)] From the results of drained shear tests under special arranged stress paths, they concluded that yield condition of sand is nearly determined by effective stress ratio $((\sigma_1-\sigma_3)/\sigma_m)$; where σ_1 and σ_3 are the major and the minor principal stress, respectively, and $\sigma_m(=(\sigma_1+2\sigma_3)/3)$ is the mean effective stress. Following in this study, the works by means of the same

* M. Eng., Central Research Institute of Electric Power Industry, Civil Engineering Laboratory.

** M. Eng., Manager, Soil Mechanics Section, Foundation and Earthquake Engineering Department, Central Research Institute of Electric Power Industry, Civil Engineering Laboratory.

experimental manner as that of Poorooshasb et al. were performed by Barden et al.[4] and Tatsuoka and Ishihara[25], and they gave qualitatively the same results as those of Poorooshasb et al.

On the other hand, Schofield and Wroth[22] advanced the deformation theory of sand called Granta gravel model based on the concept of plasticity and energy balance equation. Yield function proposed by them is given by the following equation.

$$\frac{\sigma_1-\sigma_3}{\sigma_m}+M\cdot\log_e\frac{\sigma_m}{\sigma_{my}}=0 \quad \cdots\cdots(1)$$

where M is a value defined by $(\sigma_1-\sigma_3)/\sigma_m$ at critical state and σ_{my} is a parameter that gives work hardening or work softening effect.

The different points between Eq. (1) and yield function which was experimentaly given by Poorooshasb et al. and the others are as follows.

(i) While Schofield and Wroth assumed that yield function represented in Eq. (1) coincides with the plastic potential, Poorooshasb et al. showed experimentaly that yield function is defferent from plastic potential.

(ii) Yielding behaviour for isotropic compression can be expressed by Eq. (1). However, this experimental facts can not be explained by yield function proposed by Poorooshasb et al. and Lade and Duncan[10].

Now, according to Granta gravel model, when normally consolidated or lightly overconsolidated specimens are sheared after isotropic consolidation, deformation properties of them are defined as work hardening materials with volume contraction which σ_{my} in Eq. (1) monotonously increases. On the other hand, work softening behaviour taking with volume expansion is caused at heavily overconsolidated state defined as "Dry" side by Roscoe et al. after arriving to initial yield surface prescribed with pre-consolidation pressure. This means that σ_{my} in Eq. (1) decrease monotonously after yielding.

The results of the isotropic compression tests of sand under very high stress condition generally show that remarkable yielding behaviour starts from isotropic stress state in the range of 50~100/cm^2 and the compressibility of sand is very small below this pressure. Also, for sample consolidated under such high confining pressure, the volume contracts from initial shearing state to failure state such as the behaviour of normally consolidated clay. Namely, this means that the behaviour of volume change in shear can be explained qualitatively by yield function of cap's type such as Granta gravel model. However, for comparative looser sand, plastic behaviour is caused by loading of isotropic pressure even under low confining pressure condition which may be regarded as "Dry" side. Also, deformation properties of materials with dilatancy characteristic which contracts at early stage and expands at pre-peak in shear can not be explained by construction of yield function with hardening or softening parameter represented by σ_{my}.

This is the same for heavily overconsolidated clay. Accordingly, the plastic behaviour of soils showing such dilatancy property should be discussed from the different standpoint.

3. TESTING APPARATUS AND SPECIMENS

The material used in the present investigation is a sand obtained from the bed of the Tone River. The physical properties are given in **Fig. 1** and **Table 1**. The samples tested were 12 cm in hight and 5 cm in diameter. To permit uniform deformation throughout the length of samples, two sheets of 0.25 mm thick rubber disks with lubricating silicon greese inside were placed between the sample and both end plates. The water within the specimen was free drain from the lower ends only through a 1.0 cm in diameter porous stone fixed to the center of the end plattens. The specimens were prepared by spooning freshly boiled sand into a split mold filled with de-aired water and after that by tapping the mold with a wooden hammer.

For the present study, we used a conventional

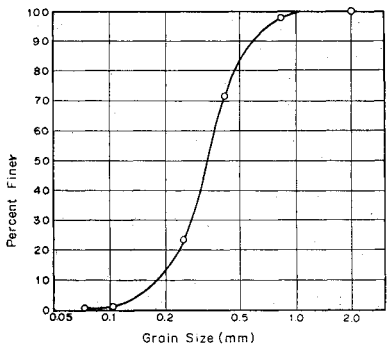

Fig. 1 Grain Size Distribution of the Sand.

Table 1 Physical Properties of Sand used in This Study.

Specific Gravity of Solids, G_s	2.701
Maximum Void Ratio, e_{max}	0.991
Minimum Void Ratio, e_{min}	0.634
Uniformity Coefficient, U_c	2.056
Effective Graine Size, D_{10} (mm)	0.18

triaxial apparatus that axial stress and radial stress independently can be loaded. All tests reported in this paper were under the drained condition and were conducted by stress control. The measured volume change for all tests that radial stress changes was corrected for membrane penetration which had been determined by the tests using brass rods having 2.0, 2.5 and 4.0 cm in diameter.

4. YIELD AND HARDENING FUNCTIONS

The following test was conducted to investigate yielding property of sand by means of the same manner as that of Poorooshasb et al. **Fig. 2** (a) and (b) illustrate the relation between effective stress ratio, i.e., the ratio of octahedral stress ratio τ_{oct} and mean effective stress σ_m, and octahedral shear strain γ_{oct}, and the relation between

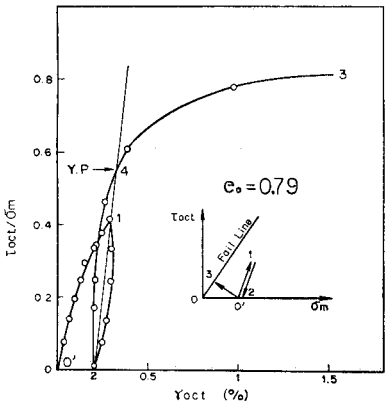

Fig. 2 (a) Relation between τ_{oct}/σ_m and γ_{oct} under the Special Repeated Loading Test.

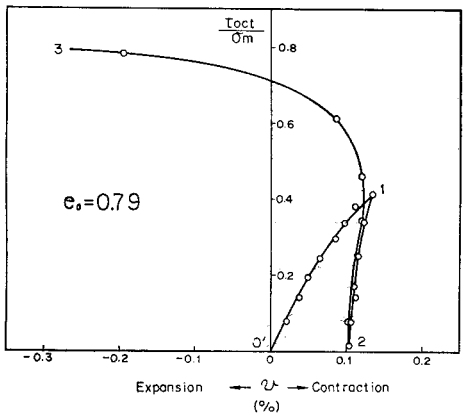

Fig. 2 (b) Relation between τ_{oct}/σ_m and v under the Special Repeated Loading Test.

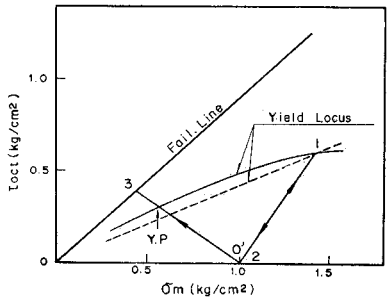

Fig. 2 (c) Yield Locus on (σ_m, τ_{oct}) Plane.

effective stress ratio and volumetric strain v which are obtained under stress path shown in right hand side in **Fig. 2** (a). In **Fig. 2** (a), remarkable plastic deformation behaviour does not seem to occur until arriving at the effective stress ratio shown as 'Y.P.' in **Fig. 2** (a), which may be regarded as yield point and is larger value than the maximum effective stress ratio (point 1) applied before. On the other hand, **Fig. 2** (b) represents that yielding for volumetric strain takes place nearly at the same effective stress ratio as that of point 1.

Though it may be difficult to determine definitely yield point from such test, if point 4 in **Fig. 2** (a) is regarded as the yield point, yield locus shown by a solid line in **Fig. 2** (c) is given. While, if one adopts the yield point that is determined from **Fig. 2** (b), the shape of yield locus nearly coincides with τ_{oct}/σ_m constant line such as shown as a broken line in **Fig. 2** (c). In any case, yield function of sand does not show that form of cap's type

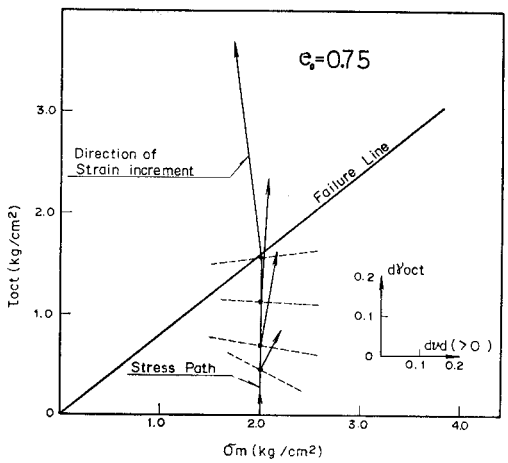

Fig. 3 Direction of Strain Increment under σ_m-const. Test.

such as Granta gravel model. It seems to show the shape such that is given almost by τ_{oct}/σ_m const. line.

Strain increments ($d\gamma_{oct}$, dv) measured under σ_m constant shear test ($\sigma_{m0}=2$ kg/cm^2) are shown on (τ_{oct}, σ_m) plane in **Fig. 3**. Volumetric strain v in **Fig. 3** is only due to dilatancy because the mean stress is kept constant. Assuming that yield surface represented in **Fig. 2** (c) is identical with plastic potential, volume change shows only expansion from starting of shear. However, actual behaviour is different from it and plastic strain increment's direction changes inversely from early stage in shear up to failure state. This general experimental results mean that associated flow rule which the yield function is identical with plastic potential function is not applicable for sand.

Fig. 4 (a) and **4** (b) show that relations between τ_{oct}/σ_m, γ_{oct} and v under stress paths shown in left hand side in **Fig. 4** (a), which are sheared from stress state of $\sigma_m=2.65$ kg/cm^2 after being consolidated under $\tau_{oct}/\sigma_m=$ const. ($=0.56$) to various stress direction. The stress paths satisfying $d(\tau_{oct}/\sigma_m)>0$ are those of $0'\rightarrow 2$, $0'\rightarrow 3$ and $0'\rightarrow 4$ if only compression side ($\sigma_1>\sigma_2=\sigma_3$) is

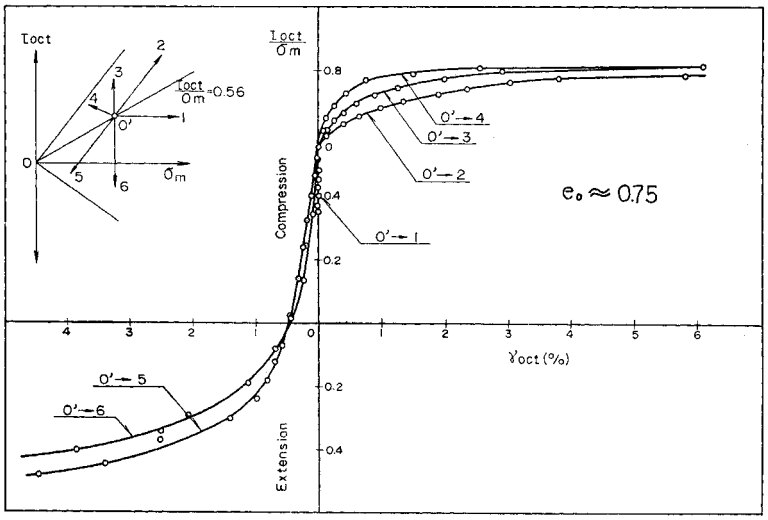

Fig. 4 (a) Relation between τ_{oct}/σ_m and γ_{oct} in Triaxial Compression and Extension Tests after Anisotropic Compression.

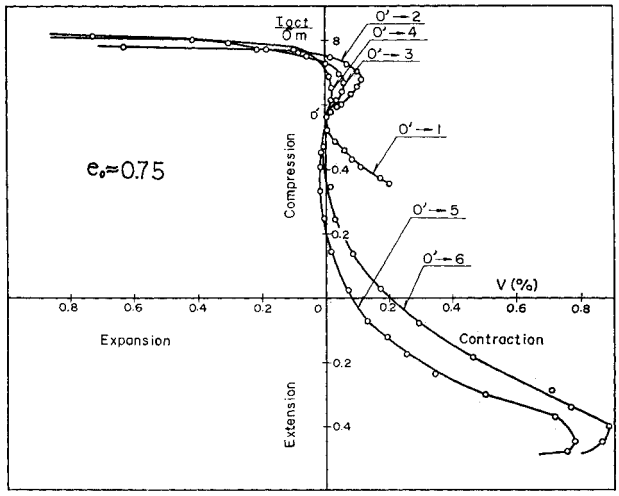

Fig. 4 (b) Relation between τ_{oct}/σ_m and v in Triaxial Compression and Extension Tests after Anisotropic Compression.

taken up. Though plastic behaviour from early stage in shear is remarkable for such stress paths, deformation behaviour of sample loaded from 0′ to 1 shows a different nature. Namely, under such stress path, shear strain equals to nearly zero and volume change only produces. As shear strain has a close relation with the dilatancy, volume change under such stress path will be regarded as one due to consolidation. The mechanism of such plastic deformation in consolidation under low confining pressure may be different from that of very high confining pressure which show the high compressibility. And for dense sand, plastic volume change due to consolidation may be negligible in comparison with plastic volume change due to dilatancy. However, in order to hold correctly dilatancy characteristics of sand under various stress paths, it is necessary to separate deformation due to hydrostatic compression into elastic and plastic component.

From above mentioned experimental results and the works of the other researchers,[14),25)] assuming that yielding behaviour for shear deformation and consolidation can be treated independently, we propose the following yield functions.

$$f_s - f_{s,y} = \tau_{oct}/\sigma_m - (\tau_{oct}/\sigma_m)_y \quad \cdots\cdots(2)$$

$$f_c - f_{c,y} = \sigma_m - (\sigma_m)_y \quad \cdots\cdots(3)$$

where functions f_s and f_c give the yield conditions that are plastic octahedral shear strain increment $d\gamma^p_{oct}>0$ and plastic volumetric strain increment due to dilatancy $dv^p_d>0$, and plastic volumetric strain increment due to consolidation $dv^p_c>0$, respectively. Although, strictly speaking, yield locus for shear of sand shows generally convex shape for σ_m-axis, we adopt approximately τ_{oct}/σ_m const. line because of the simplicity of the stress-strain relations. $f_{s,y}$ and $f_{c,y}$ are hardening parameters for shear deformation and isotropic consolidation, respectively. Hardening parameter expresses the extent of progress of plastic deformation and it generally depends on plastic strain history or stress history such as shown as the deformation behaviour which is seen in case of shearing to extension side from anisotropic consolidated state at compression side. The formulation of concrete hardening function will be conducted in later section.

5. PLASTIC POTENTIAL

As described in previous discussion on yielding properties, plastic strain increments should be divided into plastic volumetric strain increment dv^p_c which is brought above only by a increase in σ_m, and plastic octahedral strain increment $d\gamma^p_{oct}$ and plastic volumetric strain increment dv^p_d to be ascribed to dilatancy which are produced only by a increase in τ_{oct}/σ_m. Namely, even if τ_{oct}/σ_m decreases, when σ_m increase from a yield state described by $f_c - f_{c,y}=0$, dv^p_c is non negative. On the other hand, if τ_{oct}/σ_m increases from a yield state described by $f_s - f_{s,y}=0$ without increasing in σ_m, $d\gamma^p_{oct}$ and dv^p_d are non negative. According to the discussion on the occurring of the plastic strain increments, yield condition $f_c=f_{c,y}$ for consolidation process may be regarded as plastic potential because the direction of dv^p_c is parallel with σ_m-axis in (τ_{oct}, σ_m) plane. Namely, if yield condition $f_c - f_{c,y}=0$ and $df_c>0$ is only satisfied, then plastic potential is given as:

$$g_c=\sigma_m \quad \cdots\cdots(4)$$

Based on the above mentioned consideration, plastic potential for shearing process which $f_s - f_{s,y}=0$ and $df_s>0$ are satisfied should be discussed for $d\gamma^p_{oct}$, and dv^p_d obtained by subtracting volumetric strain increment dv_c due to consolidation from total volumetric strain increment dv for the stress paths that σ_m increases or decreases.

Fig. 5 (a) and **5** (b) show the relations between $dv^p_d/d\gamma^p_{oct}$ and τ_{oct}/σ_m derived from triaxial compression and extension tests, respectively, after isotropic consolidation. And **Fig. 5** (c) represents the same relations obtained by triaxial compression tests after anisotropic consolidation. Plastic volumetric strain increment dv^p_d is obtained by subtracting dv_c or dv^E_c from total volumetric strain increment dv. dv_c and dv^E_c are given by isotropic consolidation and swelling test, respectively, and it is necessary to use volumetric strain increment given by normally consolida-

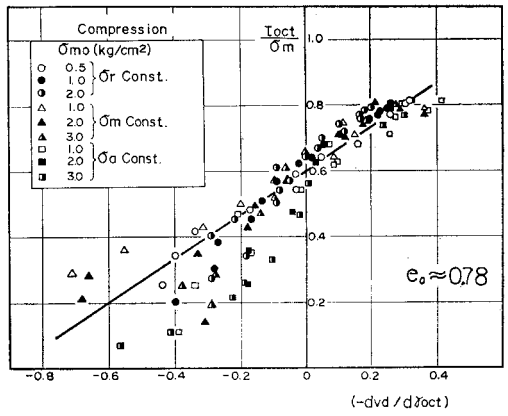

Fig. 5 (a) Relation between τ_{oct}/σ_m and $dv_d/d\gamma_{oct}$ in Triaxial Compression Tests.

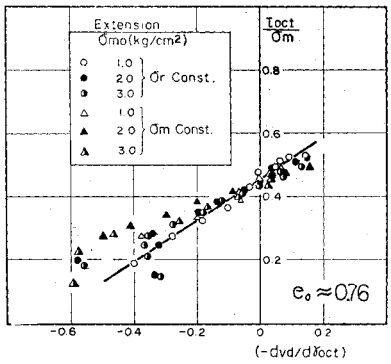

Fig. 5 (b) Relation between τ_{oct}/σ_m and $dv_d/d\gamma_{oct}$ in Triaxial Extension Tests.

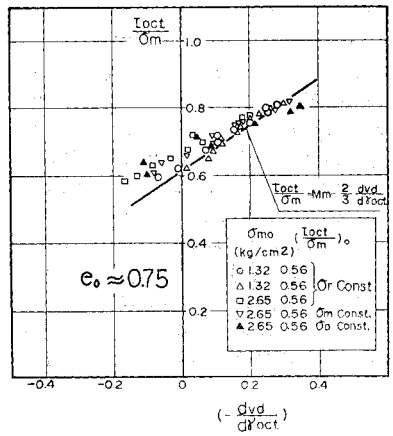

Fig. 5 (c) Relation between τ_{oct}/σ_m and $dv_d/d\gamma_{oct}$ in Triaxial Compression Tests after Anisotropic Compression.

tion curve and swelling curve in due to consideration of yield condition of consolidation for a stress state in shear.

Though $d\gamma^p_{oct}$ is given by subtracting elastic component $d\gamma^E_{oct}$ from total octahedral shear strain increment $d\gamma_{oct}$, $d\gamma^p_{oct}$ in **Fig. 5** equals to $d\gamma_{oct}$ by the reason why the estimation of $d\gamma^E_{oct}$ is difficult and it is small in comparison with $d\gamma^p_{oct}$. Also, elastic component of dv_d may be neglected, too.

Fig. 5 (a), (b) and (c) show that the relation between $dv^p_d/d\gamma^p_{oct}$ and τ_{oct}/σ_m are expressed uniquely by linear curve except at initial shear deformation. This means that the relation between $dv^p_d/d\gamma^p_{oct}$ and τ_{oct}/σ_m is determined uniquely disregarding stress paths if yield condition, $f_s-f_{s,y}=0$ and $df_{s,y}>0$ is satisfied.

Roscoe et al. gave such relations in the following equation.

$$\tau_{oct}/\sigma_m = M - \frac{2}{3}\frac{dv^p}{d\gamma^p_{oct}} \quad \cdots\cdots(5)$$

There are mainly two different points between the above equation and linear relations in **Fig. 5** (a), (b) and **5** (c). One is that dv^p in Eq. (5) is the sum of dv^p_d and dv^p_c, but dv^p in **Fig. 5** expresses dv^p_d only. Of course, if one assumes that dv^p_c is not occurred by a increase of mean effective stress σ_m, the difference is not found. Another is no agreement between compression ($\sigma_1>\sigma_2=\sigma_3$) and extension ($\sigma_1=\sigma_2>\sigma_3$) sides such as shown in **Fig. 5** (a) and **5** (b). Namely, there are difference for τ_{oct}/σ_m—value at the maximum contraction point of volume change, that is $dv^p_d=0$. This means that maximum contraction point is not given by the expression of Von-Mises's type expressed in Eq. (5), but it depends on the direction of stress, that is, the value of intermediate principal stress.

This results have already been shown by some researchers from the experiments using the true triaxial testing machine (e.g., Shimobe and Miyamori,[23] Moroto et al.[15]).

Accordingly, Eq. (5) is written by another formulation as follows:

$$\tau_{oct}/\sigma_m = M_m(b) - \frac{2}{3}\frac{dv^p_d}{d\gamma^p_{oct}} \quad \cdots\cdots(6)$$

where M_m is τ_{oct}/σ_m-value at $dv^p_d=0$ and it generally will depend on the value of intermediate principal stress expressed by b-value given by the following equation.

$$b=\frac{\sigma_2-\sigma_3}{\sigma_1-\sigma_3} \quad \cdots\cdots(7)$$

Eq. (6) shows that plastic strain increment ratio $dv^p_d/d\gamma^p_{oct}$ is determined uniquely by τ_{oct}/σ_m if the direction of stress, i.e., b-value is fixed and if yield condition is satisfied.

Then, one can obtain the following plastic potential g_s having parameter b by combining Eq. (6) and normality rule; $2/3(dv^p_d/d\gamma^p_{oct})=-d\tau_{oct}/d\sigma_m$ (See Akai, Adachi and Nishi[2]). Namely,

$$g_s=\tau_{oct}/\sigma_m+M_m(b)\cdot\log_e\sigma_m \quad \cdots\cdots(8)$$

Fig. 6 illustrates plastic potential given by Eq. (8) in (τ_{oct}, σ_m) plane. For example, when a sample of sand is sheared under σ_m constant condition after isotropic consolidation, the volume contraction occurs when τ_{oct}/σ_m is smaller than $M_m(b)$; i.e., 0′→1→2 in **Fig. 6**, and the volume expansion occurs when τ_{oct}/σ_m is larger than $M_m(b)$; i.e., 2→3→4 in **Fig. 6**, showing work hardening up to failure line. Accordingly, volume deformation property of sand showing contraction and expansion can be explained by means of such

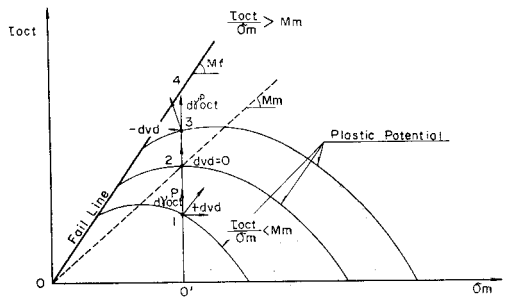

Fig. 6 Plastic Potential Expressed by Eq. (8).

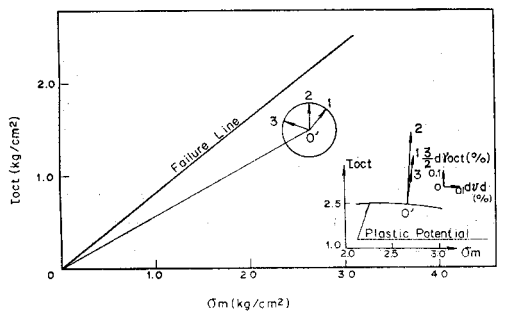

Fig. 7 Direction of Plastic Strain Increment for Plastic Potential.

plastic potential.

Fig. 7 illustrates measured plastic strain increment ($d\gamma^p_{oct}$, dv^p_d) and stress paths in shear after anisotropic consolidation. The configuration of plastic potential is also shown in **Fig. 7**. The good agreement is clear between the direction of strain increments and that of normal for plastic potential.

6. STRESS-STRAIN-RELATIONSHIPS

Total strain increments $d\varepsilon_{ij}$ ($i, j=1, 2, 3$) are assumed to be divided into elastic strain increments $d\varepsilon^E_{ij}$ and plastic strain increments $d\varepsilon^p_{ij}$ as follows:

$$d\varepsilon_{ij}=d\varepsilon^E_{ij}+d\varepsilon^p_{ij} \quad \cdots\cdots(9)$$

Elastic strain increments $d\varepsilon^E_{ij}$ are estimated by generalized Hooke's law. On the other hand, plastic strain increments $d\varepsilon^p_{ij}$ are given by the following equation (Hill[7]).

$$d\varepsilon^p_{ij}=h\frac{\partial g}{\partial\sigma_{ij}}df \quad \cdots\cdots(10)$$

where h is the function of stress and strain history, σ_{ij} is stress tensors, and g and f are plastic potential and yield functions, respectively. Using yield function f, the condition that $d\varepsilon^p_{ij}$ is non negative is expressed by the following equation.

$$f-f_y=0 \quad \text{and} \quad df>0 \quad \cdots\cdots(11)$$

If one uses the yield and plastic potential functions of sand which were previously discussed, we can easily derive stress-strain relationships by using Eq. (10) and by fixing b-value temporarily.

(I) when yield condition for shear ($f_s-f_{s,y}=0$ and $df_s>0$) is only satisfied:

$$d\varepsilon^p_{ij}=h_s\frac{\partial g_s}{\partial\sigma_{ij}}df_s$$
$$=\frac{h_s}{3\sigma_m}\left\{\left(M_m(b)-\frac{\tau_{oct}}{\sigma_m}\right)\delta_{ij}+\frac{S_{ij}}{\tau_{oct}}\right\}d(\tau_{oct}/\sigma_m) \quad \cdots\cdots(12)$$

where S_{ij} is deviatoric stress tensors ($=\sigma_{ij}-\sigma_m\delta_{ij}$) and δ_{ij} is Kronecker delta.

(II) when yield condition for consolidation ($f_c-f_{c,y}=0$ and $df_c>0$) is only satisfied:

$$d\varepsilon^p_{ij}=h_s\frac{\partial g_c}{\partial\sigma_{ij}}df_s$$
$$=h_c d\sigma_m\frac{\delta_{ij}}{3} \quad \cdots\cdots(13)$$

(III) when both yield conditions ($f_s-f_{s,y}=0$ and $df_s>0$, $f_c-f_{c,y}=0$ and $df_c>0$) are simultaneously satisfied:

$$d\varepsilon^p_{ij}=h_s\frac{\partial g_s}{\partial\sigma_{ij}}df_s+h_c\frac{\partial g_c}{\partial\sigma_{ij}}df_c$$
$$=\frac{h_s}{3\sigma_m}\left\{\left(M_m(b)-\frac{\tau_{oct}}{\sigma_m}\right)\delta_{ij}+\frac{S_{ij}}{\tau_{oct}}\right\}$$
$$\cdot d(\tau_{oct}/\sigma_m)+h_c d\sigma_m\frac{\delta_{ij}}{3} \quad \cdots\cdots(14)$$

Also, plastic octahedral shearing strain increment $d\gamma^p_{oct}$, plastic volumetric strain increment due to dilatancy dv^p_d and plastic volumetric strain increment due to consolidation dv^p_c are given as follows, respectively.

$$d\gamma^p_{oct}=\frac{2}{3}h_s\frac{\partial g_s}{\partial\tau_{oct}}df_s$$
$$=\frac{2}{3}\frac{h_s}{\sigma_m}d(\tau_{oct}/\sigma_m) \quad \cdots\cdots(15)$$

$$dv^p_d=h_s\frac{\partial g_s}{\partial\sigma_m}df_s$$
$$=\frac{h_s}{\sigma_m}\left\{M_m(b)-\frac{\tau_{oct}}{\sigma_m}d(\tau_{oct}/\sigma_m)\right\} \quad \cdots\cdots(16)$$

$$dv^p_c=h_c\frac{\partial g_c}{\partial\sigma_m}df_c$$
$$=h_c d\sigma_m \quad \cdots\cdots(17)$$

7. VERIFICATION OF STRESS-STRAIN RELATIONSHIPS

(1) Definite expression of hardening function

To express the expansion of elastic limit that accompanies plastic deformation, hardening function have to be given definitely. Here, we assume isotropic hardening as a first step which yield surface expands isotropically in stress space in proportion to progress of plastic deformation. And we set up the following hardening function by assuming that the extent of hardening can be expressed by plastic octahedral shear strain and plastic volumetric strain due to consolidation for each of yielding behaviour of shear and consolidation.

$$(\tau_{oct}/\sigma_m)_y = F_s\left(\int d\gamma^p_{oct}, b\right) \quad \cdots\cdots(18)$$

$$(\sigma_m)_y = F_c\left(\int dv^p_c\right) \quad \cdots\cdots(19)$$

The reason why introduces b-value in Eq. (18) is that the hardening behaviour under a stress state with one b-value can not be explained by the same hardening function as that of a stress state with the different b-value. For example, stress-strain curve and failure value are different due to intermediate principal stress such as triaxial compression ($b=0$) and extension ($b=-1$) side.

Concretely, for the former, it is assumed that a hyperbolic curve using effective stress ratio at failure state $(\tau_{oct}/\sigma_m)_f$ which generally depends on the b-value and the initial tangent modulus G' in $\tau_{oct}/\sigma_m - \gamma^p_{oct}$ curve. It is not necessary to express $\tau_{oct}/\sigma_m - \gamma^p_{oct}$ curve by a hyperbolic one, however the hardening function can be easily formulated by this expression in terms of two basic parameter of soils. Namely, the relation between τ_{oct}/σ_m and γ^p_{oct} is given by the following equation.

$$\tau_{oct}/\sigma_m = \frac{\gamma^p_{oct}}{(G')^{-1}+[M_f(b)]^{-1}\gamma^p_{oct}} \quad \cdots\cdots(20)$$

where $(\tau_{oct}/\sigma_m)_f = M_f(b)$.

Here, it is assumed that G' is not dependent on b-value, but it depends on initial confining pressure σ_{m0}. $\tau_{oct}/\sigma_m - \gamma^p_{oct}$ curves for Tone River sand under σ_m-constant condition ($\sigma_{m0}=2.0$ kg/cm^2) in triaxial compression and extension sides are illustrated in **Fig. 8**. The test results by using true triaxial testing machine (Miyamori et al.[13]) are also shown in **Fig. 9**, which were obtained by σ_m-constant tests that varied the direction of stress after isotropic consolidation. From these test results, it is known that assumption for the independency on b-value of G' may be allowable. However, G' is generally affected by initial confining pressure σ_{m0} as shown in **Fig. 10**, which were obtained by triaxial compression tests under radial stress constant condition.

From **Fig. 10**, we can formulate G' as the function of initial confining pressure and void ratio by the following equation.

$$G' = \frac{1}{\sigma_{m0}} KP_a\left(\frac{\sigma_{m0}}{P_a}\right)^n \quad \cdots\cdots(21)$$

where P_a is the atmospheric pressure, and K and n are material constants depending on void ratio. $\sigma_{m0}G'$ is equivalent with the expression of Young's modulus proposed by Janbu.[8]

Now, let's consider to extend $M_f(b)$ and $M_m(b)$ in Eq. (8) and Eq. (20), to generalized stress conditions. There have been many works on failure

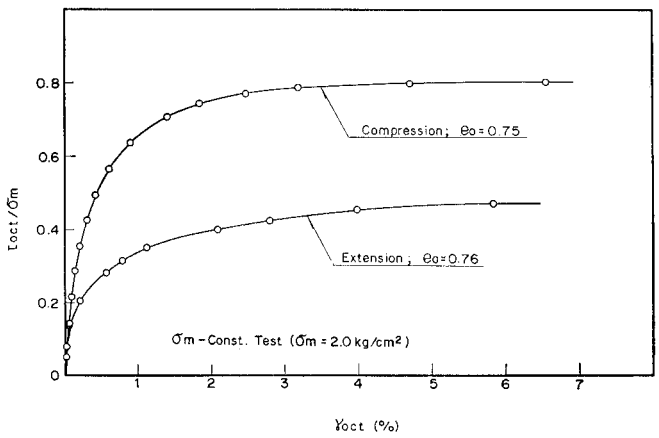

Fig. 8 Relation between τ_{oct}/σ_m and γ_{oct} in Triaxial Compressi on and Extension Tests (Hardening Curves).

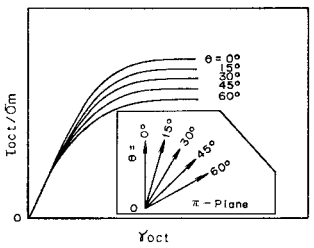

Fig. 9 Relation between τ_{oct}/σ_m and γ_{oct} in True Triaxial Tests (after Miyamori et al. (1974)).

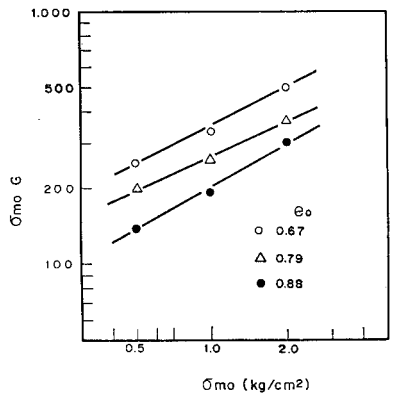

Fig. 10 Relation between G' and Initial Confining Pressure σ_{mo}.

criteria for sand and it is said that it is influenced by the density and the direction of stress, i.e., intermediate principal stress. From the experimental data using true triaxial testing machine, various failure criteria are proposed by many investigators, Bishop,[5] Lade and Duncan,[9] Matsuoka[12] and the others. A lot of these are critical for more popular failure criterion, i.e., Mohr Coulomb criterion. However, test results may be influenced by loading methods and defects of testing machine, particularly the friction of loading plate. As actual problem, tests using true triaxial testing machine are not practical. Also, Mohr Coulomb criterion is expected to give the value of safety side. Accordingly, in this paper using Mohr Coulomb criterion as the initial step, hardening and plastic potential functions are formulated.

Mohr Coulomb criterion is given by the following relation for cohensionless materials.

$$\frac{\sigma_1-\sigma_3}{\sigma_1+\sigma_3}=\sin\phi \quad \cdots\cdots(22)$$

where ϕ is the angle of internal friction.

When Eq. (22) and b-value given in Eq. (7) are used, $M_f(b)$ and $M_m(b)$ are expressed as follows, respectively.

$$M_f(b)=\left(\frac{\tau_{oct}}{\sigma_m}\right)_f=\frac{\sqrt{(\sigma_1-\sigma_2)^2+(\sigma_2-\sigma_3)^2+(\sigma_3-\sigma_1)^2}}{\sigma_1+\sigma_2+\sigma_3}=\frac{2\sqrt{2}\sin\phi_f\sqrt{b^2-b+1}}{3+(2b-1)\sin\phi_f} \quad \cdots\cdots(23)$$

$$M_m(b)=\left(\frac{\tau_{oct}}{\sigma_m}\right)_m=\frac{2\sqrt{2}\sin\phi_m\sqrt{b^2-b+1}}{3+(2b-1)\sin\phi_m} \quad \cdots\cdots(24)$$

where ϕ_f and ϕ_m are the angle of internal friction at failure state and at maximum contraction point $dv_d=0$, respectively.

Now, using Eq. (15) and Eq. (20), h_s is given as

$$\frac{3\sigma_m}{2G'}\left(\frac{M_f(b)}{M_f(b)-\tau_{oct}/\sigma_m}\right) \quad \cdots\cdots(25)$$

On the other hand, the relation between v_c and σ_m are obtained by assuming the lineality of e-log σ_m curve. Namely,

$$e=e_1-\lambda\cdot\log\sigma_m \quad \cdots\cdots(26)$$

$$e^E=e_1'-\kappa\cdot\log\sigma_m \quad \cdots\cdots(27)$$

where λ and κ are slopes of normally consolidated curve and swelling curve, respectively, and e_1 and e_1' are the void ratio at $\sigma_m=1.0$ kg/cm. From Eq. (26) and Eq. (27), the following equation is derived.

$$dv_c^p=\frac{-de^p}{1+e}=\frac{\lambda-\kappa}{1+e}\frac{d\sigma_m}{\sigma_m} \quad \cdots\cdots(28)$$

Using Eq. (17) and Eq. (28), h_c is expressed by the following equation.

$$h_c=\frac{\lambda-\kappa}{1+e}\frac{1}{\sigma_m} \quad \cdots\cdots(29)$$

(2) Verification of stress-strain relationships

To evaluate the ability of the elasto-plastic work-hardening model to predict stress-strain behaviour of sand, verification is performed by using the results of conventional triaxial tests.

Fig. 11 represents the data of triaxial compression tests ($\sigma_{m0}=2.0$ kg/cm²) and triaxial extension tests ($\sigma_{m0}=2.0$ kg/cm²) which were conducted under various stress conditions and the curves of values calculated from Eq. (12)~Eq. (14). In the calculations, $G'=250$, $\phi_f=40.8°$, $\phi_m=32.9°$, $\lambda=0.0062$ and $\kappa=0.0013$ were used for the results for each tests. **Fig. 12** represents the data of triaxial compression test after an-

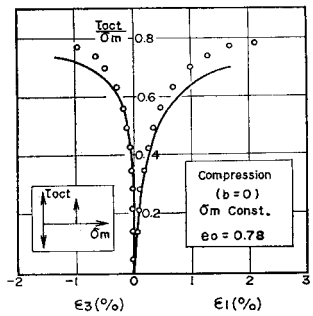

Fig. 11 (a) Relation among τ_{oct}/σ_m, ϵ_1 and ϵ_3 in Triaxial Compression Test under σ_m-constant Condition.

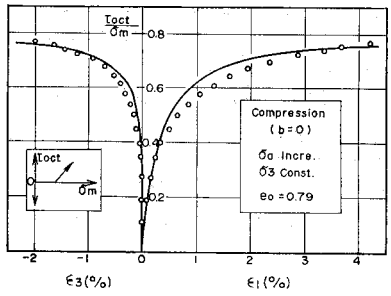

Fig. 11 (b) Relation among τ_{oct}/σ_m, ϵ_1 and ϵ_3 in Triaxial Compression Test under Lateral Stress Constant Condition.

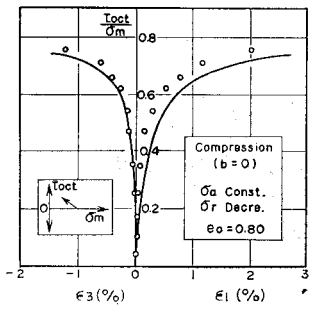

Fig. 11 (c) Relation among τ_{oct}/σ_m, ϵ_1 and ϵ_3 in Triaxial Compression Test under Axial Stress Constant Condition.

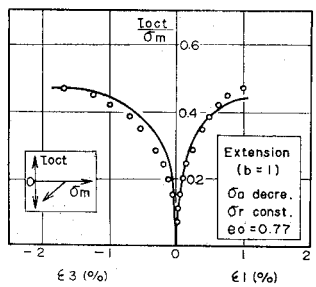

Fig. 11 (d) Relation among τ_{oct}/σ_m, ϵ_1 and ϵ_3 in Triaxial Extension Test under Lateral Stress Constant Condition.

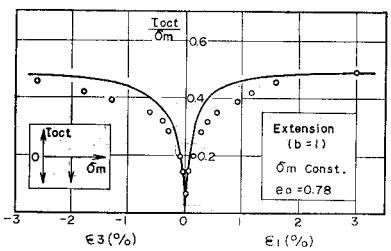

Fig. 11 (e) Relation among τ_{oct}/σ_m, ϵ_1 and ϵ_3 in Triaxial Extension Test under σ_m-constant Condition.

isotropic consolidation ($\sigma_{m0}=2.65$ kg/cm^2, $(\tau_{oct}/\sigma_m)_0=0.56$) and the curves of values calculated from Eq. (14). This test data was obtained under radial stress ($=\sigma_3$)-constant condition. The coefficients used are the same as those of theoretical curves in **Fig. 11**. The strain predicted for the tests with the different b-values and stress paths are reasonably accurate. Also, proposed model can successfully predict the strains for the tests with the different consolidation states.

Fig. 13 and **14** show the data of triaxial compression tests for looser sand ($\sigma_{m0}=1.0$ kg/cm^2 and $e=0.88$) and denser sand ($\sigma_{m0}=1.0$ kg/cm^2 and $e=0.67$) which were performed under the condition of radial stress constant and the curves of values calculated from Eq. (14), respectively. In the calculation, $G'=192.3$, $\phi_f=38.4°$, $\phi_m=33.6°$, $\lambda=0.0098$ and $\kappa=0.0010$ for looser sand, and $G'=333.0$, $\phi=49.4°$, $\phi_m=32.6°$, $\lambda=0.0058$ and $\kappa=0.0028$ for denser sand were used. The agreement between the experimental and theoretical results for looser and denser sand is satisfactory.

Thus, it can be concluded that the proposed elasto-plastic model can effectively represent the

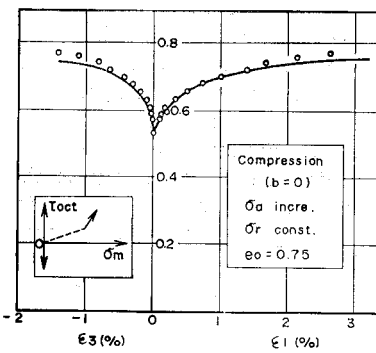

Fig. 12 Relation among τ_{oct}/σ_m, ϵ_1 and ϵ_3 in Triaxial Compression Test after Anisotropic Compression Test.

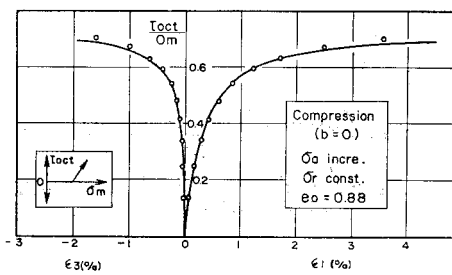

Fig. 13 Relation among τ_{oct}/σ_m, ϵ_1 and ϵ_3 in Triaxial Compression Test.

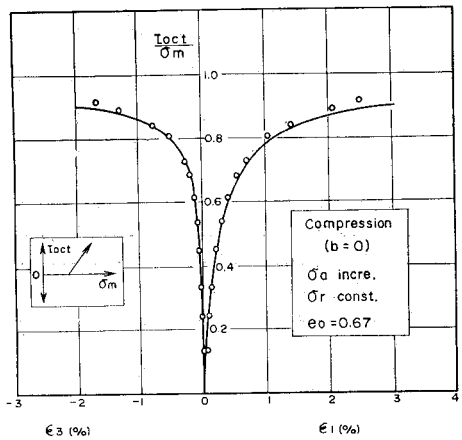

Fig. 14 Relation among τ_{oct}/σ_m, ϵ_1 and ϵ_3 in Triaxial Compression Test.

mechanical behaviour of sand under the triaxial stress state ($b=1.0$ and 0). It is remained as the future works to verify the test results under plane strain and triaxial stress state and to model the plastic deformation in the anisotropic consolidation and under the cyclic loading.

8. CONCLUDING REMARKS

Stress-strain relationships of sand under generalized stress conditions are derived with the help of the concept of non-associated flow rule based on the elasto-plasticity theory. The proposed elasto-plastic work hardening model produces reasonably close agreement with the experimental results. Accordingly, it would be possible to predict complicated response of sand showing dilatancy and stress path effect. The application of the analysis to boundary value problems using the proposed model will be published in the near future.

ACKNOWLEDGEMENT

The authors wish to thank our superviser Dr. Masao Hayashi of Central Research Institute of Electric Power Industry for his valuable guidance, and Mr. Kaname Takahashi for his able assistance in the laboratory.

REFERENCES

1) Adachi, T. and Okano, M.: A constitutive equation for normally consolidated clay, Soils and Foundations, Vol. 14, No. 4, pp. 55–73, 1974.
2) Akai, K., Adachi, T. and Nishi, K.: Mechanical properties of soft rocks, Proc. 9th Int. Conf. Soil Mech. Found. Eng., Vol. 1, pp. 7–10, 1977.
3) Barden, L. and Khayatt, A. J.: Incremental strain rate ratios and strength of sand in the triaxial test, Geotechnique, Vol. 16, No. 4, pp. 338–357, 1966.
4) Barden, L., Ismail, H. and Tong, P.: Plane strain deformation of granular material at low and high pressure, Geotechnique, Vol. 19, No. 4, pp. 441–452, 1969.
5) Bishop, A. W.: The strength of soils as engineering materials, Geotechnique, Vol. 16, No. 2, pp. 91–128, 1966.
6) Duncan, J. M. and Chang, C. Y.: Nonlinear analysis of stress and strain in soils, Proc. ASCE, SM 5, pp. 1629–1653, 1970.
7) Hill, R.: The Mathematical Theory of Plasticity, Oxford Univ. Press, London, 1950.
8) Janbu, N.: Soil compressibility as determined by oedometer and triaxial tests, Proc. Europäishe Baugrundtagung, pp. 19–25, 1963.
9) Lade, P. V. and Duncan, J. M.: Cubical triaxial tests on cohesionless soil, Proc. ASCE, SM 10, pp. 793–812, 1973.
10) Lade, P. V. and Duncan, J. M.: Elasto-plastic stress-strain theory for cohesionless soil, Proc. ASCE, GT 10, pp. 1037–1053, 1975.
11) Matsuoka, H.: Stress-strain relationships of sands based on the mobilized plane, Soils and Foundations, Vol. 14, No. 2, pp. 47–61, 1974.
12) Matsuoka, H.: "On the significance of the "spatial mobilized plane," Soils and Foundations, Vol. 16, No. 1, pp. 91–100, 1976.
13) Miyamori, T. and Shimobe, S.: True triaxial tests on a dry sand (2nd report), Proc. 29th Annual meeting of JSCE, Part 3, pp. 33–34, (in Japanese), 1974.
14) Moroto, N. and Kawakami, F.: State function of sand deformation, Proc. JSCE, No. 229, pp. 77–86, (in Japanese), 1974.
15) Moroto, N., Oikawa, K. and Okamoto, T.: Behaviour of sand under the three principal stress state, Proc. 30th Annual Meeting of JSCE, Part 3, pp. 13–14, (in Japanese), 1975.
16) Murayama, S.: A theoretical consideration on a behaviour of sand, Proc. IUTAM Rheology and Soil Mechanics Symposium,

Grenoble, pp. 146–157, 1964.

17) Poorooshasb, H. B., Holubec, I. and Sherbourne, A. N.: Yielding and flow of sand in triaxial compression, part I, Canadian Geotechnical Journal, Vol. 3, No. 4, pp. 179–190, 1966.

18) Poorooshasb, H. B., Holubec, I. and Sherbourne, A. N.: Yielding and flow of sand in triaxial compression, part II and III, Canadian Geotechnical Journal, Vol. 4, No. 4, pp. 377–398, 1967.

19) Poorooshasb, H. B.: Deformation of sand in triaxial compression, Proc. 4th Asian Regional Conf. on Soil Mechanics and Foundation Engineering, Bangkok, Vol. 1, pp. 63–66, 1961.

20) Roscoe, K. H., Schofield, A. N. and Thurayrajah, A.: Yielding of clays in states wetter than critical, Geotechnique, Vol. 13, pp. 211–240, 1963

21) Roscoe, K. H. and Burland, J. B.: On the generalized stress-strain behaviour of 'Wet' clay, Engineering Plasticity, Cambridge University Press, pp. 535–609, 1968.

22) Schofield, A. N. and Wroth, C. P.: Critical State Soil Mechanics, McGraw-Hill, London, 1968.

23) Shimobe, S. and Miyamori, T.: True triaxial tests on a dry sand (3rd report), Proc. 30th Annual Meeting of JSCE, Part 3, pp. 21–22, (in Japanese), 1975.

24) Simpson, M. A. and Wroth, C. P.: Finite element computations for a model retaining wall in sand, Proc. 5th European Conference on SMFE, 1972.

25) Tatsuoka, F. and Ishihara, K.: Yielding of sand in triaxial compression, Soils and Foundations, Vol. 14, No. 2, pp. 63–76, 1974.

(Received March 8, 1978)